



## Causal influence of gamma oscillations on the sensorimotor rhythm

Moritz Grosse-Wentrup<sup>\*</sup>, Bernhard Schölkopf, Jeremy Hill

Max-Planck Institute for Biological Cybernetics, Spemannstr. 38, 72076 Tübingen, Germany

### ARTICLE INFO

#### Article history:

Received 30 November 2009

Revised 26 March 2010

Accepted 30 April 2010

Available online 6 May 2010

#### Keywords:

Gamma rhythms

Sensorimotor rhythm

Causal inference

Brain–computer interfaces

Motor imagery

BCI-illiteracy

### ABSTRACT

Gamma oscillations of the electromagnetic field of the brain are known to be involved in a variety of cognitive processes, and are believed to be fundamental for information processing within the brain. While gamma oscillations have been shown to be correlated with brain rhythms at different frequencies, to date no empirical evidence has been presented that supports a *causal influence* of gamma oscillations on other brain rhythms. In this work, we study the relation of gamma oscillations and the sensorimotor rhythm (SMR) in healthy human subjects using electroencephalography. We first demonstrate that modulation of the SMR, induced by motor imagery of either the left or right hand, is positively *correlated* with the power of frontal and occipital gamma oscillations, and negatively *correlated* with the power of centro-parietal gamma oscillations. We then demonstrate that the most simple causal structure, capable of explaining the observed correlation of gamma oscillations and the SMR, entails a *causal influence* of gamma oscillations on the SMR. This finding supports the fundamental role attributed to gamma oscillations for information processing within the brain, and is of particular importance for brain–computer interfaces (BCIs). As modulation of the SMR is typically used in BCIs to infer a subject's intention, our findings entail that gamma oscillations have a causal influence on a subject's capability to utilize a BCI for means of communication.

© 2010 Elsevier Inc. All rights reserved.

### Introduction

Higher-frequency oscillations of the electromagnetic field of the brain, known as  $\gamma$  oscillations, have been associated with a diversity of cognitive processes including attention (Bauer et al., 2006; Gruber et al., 1999; Sokolov et al., 2004), short-term memory (Tallon-Baudry et al., 1998, 1999; Jokisch and Jensen, 2007), motor control (Crone et al., 1998; Pfurtscheller et al., 2003), and the integration of different object features into a coherent percept (Engel et al., 2001; Tallon-Baudry and Bertrand, 1999). One explanation for the ubiquity of  $\gamma$  rhythms in cognitive processes is provided by the hypothesis that  $\gamma$  rhythms constitute a fundamental mechanism of cortical information processing, dynamically routing signals within a fixed anatomical network (Fries et al., 2007). This hypothesis has gained further support by recent evidence that  $\gamma$  oscillations are indeed linked to performance in behavioral paradigms, providing information on successful encoding of new verbal- (Sederberg et al., 2007) and declarative memories (Osipova et al., 2006). It remains unclear, however, how  $\gamma$  rhythms interact with other brain rhythms. While recent studies have demonstrated cross-frequency *correlations* of  $\gamma$  rhythms with electromagnetic oscillations at different frequencies (Osipova et al., 2008; Canolty et al., 2006; Darvas et al., 2009; de Lange

et al., 2008), to date there is no direct evidence for a *causal influence* of  $\gamma$  oscillations on other brain rhythms.

In this work, we study the relation of  $\gamma$  oscillations and the sensorimotor rhythm (SMR) in healthy human subjects using electroencephalography (EEG). The SMR is of particular importance for research on brain–computer interfaces (BCIs), as modulation of the SMR, typically induced by motor imagery (Pfurtscheller and Neuper, 2001), constitutes the most frequently used paradigm in research on BCIs (Mason et al., 2007). We first demonstrate that modulation of the SMR, induced by motor imagery of either the left or right hand, is positively correlated with the power of frontal and occipital  $\gamma$  oscillations, and negatively correlated with the power of centro-parietal  $\gamma$  oscillations. We then proceed to investigate the causal relation of the SMR and  $\gamma$  oscillations, based on the framework for causal inference developed by Pearl, Spirtes, and others (Pearl, 2000; Spirtes et al., 2000). Specifically, we investigate the dependency structure of our empirical observations, and present strong evidence that the observed dependence of  $\gamma$  oscillations and the SMR has been generated by a causal structure in which  $\gamma$  oscillations exert a causal influence on the SMR. We thereby present the first empirical evidence for a cross-frequency *causal influence* of  $\gamma$  oscillations on other brain rhythms, which supports the fundamental role attributed to  $\gamma$  oscillations for information processing within the brain.

Our findings are furthermore of particular significance for research on BCIs based on motor imagery. Since in BCIs modulation of the SMR is typically used to infer a subject's intention, our findings entail that  $\gamma$  oscillations have a causal influence on a subject's capability to utilize a

<sup>\*</sup> Corresponding author.

E-mail addresses: [moritzgw@ieee.org](mailto:moritzgw@ieee.org) (M. Grosse-Wentrup), [bernhard.schoelkopf@tuebingen.mpg.de](mailto:bernhard.schoelkopf@tuebingen.mpg.de) (B. Schölkopf), [jez@tuebingen.mpg.de](mailto:jez@tuebingen.mpg.de) (J. Hill).

BCI for means of communication. We thereby provide the first non-trivial neurophysiological explanation for the large variation of BCI-performance across subjects, which we consider to be crucial for addressing the problem of “BCI-illiteracy”, i.e., the incapability of about 20% of subjects to reliably communicate by means of a BCI (Popescu et al., 2008). Specifically, our results indicate that subjects should be trained to volitionally shift  $\gamma$  power from centro-parietal to frontal and occipital regions in order to learn how to communicate by means of a BCI.

## Methods

### Experimental paradigm

Subjects participated in an experiment consisting of right- and left-hand motor imagery. Subjects were placed in a dimly-lit and shielded room, approximately 1.5 m in front of a screen. Each trial started with a centrally-displayed fixation cross. After three seconds, the fixation cross was superimposed by an arrow pointing either to the left or to the right, instructing subjects to initiate haptic motor imagery of the left (class label  $-1$ ) or right hand (class label  $+1$ ), respectively. The arrow was removed after further seven seconds, indicating the end of one trial and instructing subjects to cease motor imagery. A total of 150 trials per class were recorded for each subject in pseudo-randomized order.

### Data acquisition

Ten healthy subjects participated in the experiment (two female,  $25.6 \pm 2.5$  years old, eight right-handed). One subject (S3) had already participated twice in a motor imagery experiment. All other subjects had no previous experience with motor imagery or brain-computer interfaces. No feedback was provided to the subjects during the course of the experiment. During the experiment, a 128-channel electroencephalogram (EEG) was recorded at 500 Hz sampling rate using four BrainAmp amplifiers (BrainProducts GmbH, Munich). Electrodes were placed on the scalp according to the extended 10–20 system with electrode Cz used as the initial reference. EEG data was temporally filtered using a high-pass filter with a time constant of 10 s. For each subject, electrode impedances were below 10 k $\Omega$  at the start of the experiment.

### Data pre-processing

For each subject, we spatially filtered all channels of recorded EEG data using a center-surround spatial sharpening filter or *surface Laplacian* (McFarland et al., 1997). For each subject, trial, and spatially filtered recording channel, we then estimated logarithmic bandpower (using Welch's method) in the last seven seconds of each trial, corresponding to the phase during which motor imagery was actually performed, in frequency bands of 2 Hz width ranging from 7 to 85 Hz. We performed no baseline correction, since baseline correction would remove any non-task-specific modulatory effects. For the group-level analysis, we standardized the logarithmic bandpower values of each subject, channel and frequency band across the trials that comprised that subject's dataset, and then pooled all trials across subjects, resulting in a total of 3000 trials.

### SMR lateralization score

In order to cope with the between-subject variation, we chose a machine learning approach to compute the SMR. Specifically, we used

a linear support vector machine (SVM) to classify the data segments according to whether they corresponded to imagined left- or right-hand movements. The input to the classifier consisted of logarithmic bandpower features in the range of 7–40 Hz. We employed a leave-one-trial-out procedure, in which we successively put each trial aside and used the features of the remaining trials to learn the weight vector of a linear SVM. Specifically, this was a  $\nu$  support vector classifier (Schölkopf et al., 2000), whose regularization parameter  $\nu$  was found by 10-fold cross-validation within the 299-trial training set each time. For the group-level analysis, we performed a 10-fold cross-validation rather than a leave-one-trial-out procedure due to computational resources. The resulting weight vector was then applied to the feature vector of the left-out trial(s). We thereby obtained a *continuous-valued* score for each of the 300 trials of a given subject's dataset, or for each of the 3000 trials in the group-level analysis. This score is subsequently termed the *SMR lateralization score*, as its sign is predictive of whether the trial is a left-hand (class label  $-1$ ) or right-hand (class label  $+1$ ) trial and its absolute value reflects the extent of SMR lateralization. Subjects' capability to modulate their SMR was assessed by computing the mean classification accuracy, i.e., the percentage of trials in which the sign of the SMR lateralization score coincided with the true class label.

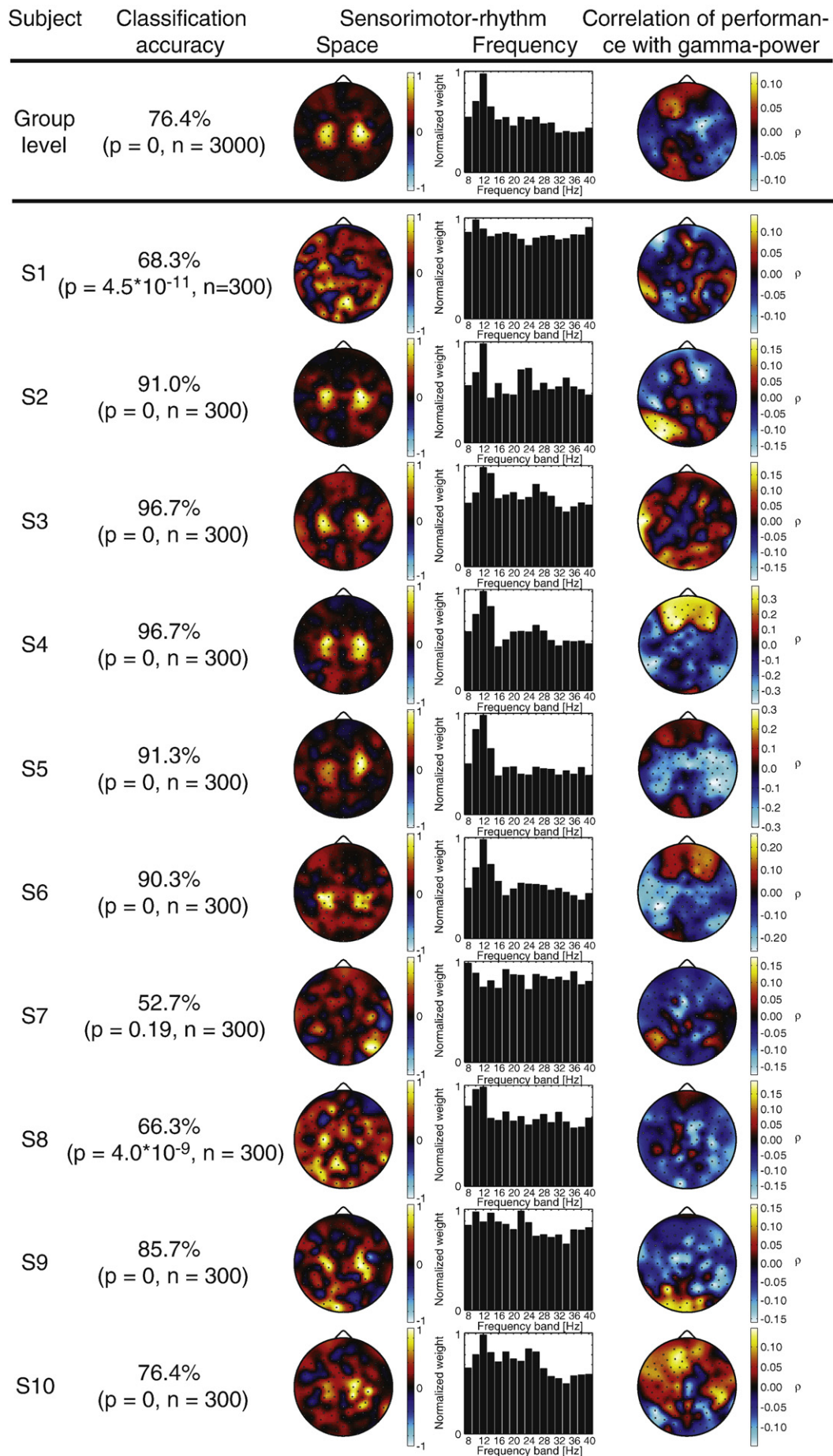
### SMR quality score

To obtain a *trial-wise* measure of how successfully subjects modulated their SMR, we multiplied the SMR lateralization score (positive for trials interpreted as right-, and negative for trials interpreted as left-hand motor imagery) by the *intended* class label, i.e.  $+1$  for trials on which the subject was instructed to perform right-hand imagery, and  $-1$  for trials on which the instruction was to perform left-hand imagery. A large positive value of the resulting *SMR quality score* therefore indicates good, easily detectable motor-imagery performance, a small value indicates undetectable motor imagery, and a negative score would indicate motor imagery that would actually be interpreted as the wrong class.

### Correlation analysis

To investigate potential relations of  $\gamma$  oscillations with the extent of SMR modulation, we computed Pearson's correlation coefficients between the leave-one-out-estimated SMR quality score and broad-band (55–85 Hz)  $\gamma$  power at each recording channel, resulting in a topographic correlation map of  $\gamma$  power and SMR modulation. Note that the definition of the  $\gamma$  band (in terms of lower and upper frequencies) varies substantially in the literature. We chose 55 Hz as the lower bound to avoid contamination by line noise and an arbitrary upper bound of 85 Hz. In order to avoid multiple comparisons in testing for a significant dependence of  $\gamma$  oscillations and the SMR, we computed a global measure of  $\gamma$  power, weighted according to the topographic correlation map. Specifically, we successively used all except one trial to compute Pearson's correlation coefficients of the SMR quality score with  $\gamma$  power at each recording channel, and then linearly combined the resulting coefficient vector with the vector of  $\gamma$  power across channels in the remaining trial. We thereby obtained 300 scalar values for each single-subject analysis (or 3000 for the group-level analysis), corresponding to a global measure of  $\gamma$  power correlated with SMR modulation. Subsequent statistical tests in the [Correlation of  \$\gamma\$  oscillations and SMR modulation](#) section as well as in the [Causal influence of  \$\gamma\$  oscillations on SMR modulation](#) section refer to this global measure of  $\gamma$  power.

**Fig. 1.** Subject-specific classification accuracies and associated  $p$ -values (second column), spatial and spectral features of the sensorimotor rhythm (third and fourth column), and topographies of Pearson's correlation coefficients of broad-band  $\gamma$  power and subject performance as measured by the SMR quality score (fifth column).





## Statistical analysis

To test for statistically significant SMR modulation (i.e. classification accuracy), we employed a binomial distribution to test the null-hypothesis that classification accuracy  $P_e$  does not exceed chance level, i.e.,  $H_0: P_e = 50\%$ . Statistical significance of Pearson's correlation coefficients was assessed by performing a permutation analysis with  $n_p = 10^4$  permutations after rejecting outliers not within two standard deviations of the sample median. Non-linear independence tests in the [Causal influence of  \$\gamma\$  oscillations on SMR modulation](#) section were based on the Hilbert–Schmidt independence criterion (HSIC) (Gretton et al., 2008). The HSIC test utilizes a kernel independence measure, capable of detecting linear as well as non-linear dependencies between arbitrary input variables. The  $p$ -values of the HSIC tests were computed using a permutation analysis with  $n_p = 10^4$  permutations. The kernel size for the HSIC tests was set to the median distance between points in input space (Gretton et al., 2008).

## Results

In order to assess the subjects' capability to modulate their SMR, we computed group-level as well as single-subject classification accuracies (percentage of trials in which the sign of the SMR lateralization score corresponds to the intended movement imagination) and associated  $p$ -values for rejecting the null-hypothesis that classification accuracy equals chance level (second column of Fig. 1). With the exception of subject S7, all subjects performed significantly above chance level, with  $p$ -values close to or below the limits of 64-bit precision. Classification results were also found to be highly significant on the group level (top row of Fig. 1). The third and fourth column of Fig. 1 show the subject-specific weighting assigned by the SVM training procedure to each recording channel and frequency band: these were obtained by averaging the absolute values of the weighting coefficients over frequency or over electrodes, respectively. In agreement with previous reports in literature on the SMR (Pfurtscheller and Neuper, 2001), logarithmic bandpower over sensorimotor areas in the so-called  $\mu$  band (roughly 9–14 Hz), and to a smaller extent in the  $\beta$  frequency range (roughly 20–35 Hz), provided most information on the type of motor imagery performed by a subject in a certain trial.

Having established that, with the exception of subject S7, subjects were capable of intentionally modulating their SMR, we first present single-subject as well as group-level results correlating  $\gamma$  power with SMR modulation. We then proceed to present evidence that  $\gamma$  power is not only correlated with SMR modulation, but does indeed exert a causal influence on it.

### Correlation of $\gamma$ oscillations and SMR modulation

Topographic maps of Pearson's correlation coefficients between the SMR quality score and bandpower in the  $\gamma$  range (55–85 Hz) are shown in the fifth column of Fig. 1. On the group level (top row), this revealed a distinct spatial structure with frontal and occipital  $\gamma$  power positively correlated and centro-parietal  $\gamma$  power negatively correlated with the SMR quality score. This structure is also readily visible in the scalp maps of three out of ten subjects (S4–S6). Statistical tests for significant correlation (as described in the [Methods](#) section) rejected the null-hypothesis that the SMR quality score and  $\gamma$  power were uncorrelated at significance level  $\alpha = 0.01$  on the group level ( $\rho_{\text{Group}} = 0.0786$ ,  $p_{\text{Group}} = 9.998 \times 10^{-5}$ ,  $n = 3000$ ) as well as for subjects S1, S3, S4, S5, and S6 on the single-subject level ( $\rho_{S1} = -0.2680$ ,  $p_{S1} = 9.998 \times 10^{-5}$ ;  $\rho_{S2} = 0.0809$ ,  $p_{S2} = 0.0904$ ;  $\rho_{S3} = 0.1674$ ,  $p_{S3} = 0.0026$ ;  $\rho_{S4} = 0.3715$ ,  $p_{S4} = 9.998 \times 10^{-5}$ ;  $\rho_{S5} = 0.1834$ ,  $p_{S5} = 0.0008$ ;  $\rho_{S6} = 0.1621$ ,  $p_{S6} = 0.0028$ ;  $\rho_{S7} = -0.0062$ ,  $p_{S7} = 0.4579$ ;  $\rho_{S8} = 0.0267$ ,  $p_{S8} = 0.3326$ ;  $\rho_{S9} = 0.0667$ ,  $p_{S9} = 0.1341$ ;  $\rho_{S10} = 0.0417$ ,  $p_{S10} = 0.2355$ ,  $n = 300$  for all single-subject tests). We hence found a highly significant correlation of

SMR modulation and  $\gamma$  power on the group level as well as in five out of ten subjects on the single-subject level.

### Causal influence of $\gamma$ oscillations on SMR modulation

The observed correlation of  $\gamma$  power and the SMR quality score is not sufficient to establish a causal influence of  $\gamma$  oscillations on the SMR. However, this causal influence can be determined (according to the framework for causal inference developed by Pearl, Spirtes and others (Pearl, 2000; Spirtes et al., 2000)) by investigating which causal structures are not supported by the empirical evidence. Let  $\mathcal{V} = \{c, \text{SMR}_i, \gamma\}$  the set of variables between which we wish to identify cause–effect relations, with  $c$  denoting the instruction given to the subject, i.e.,  $c \in \{-1, +1\}$  representing motor imagery of the left or right hand,  $\text{SMR}_i$  the SMR lateralization score as discussed in the [Methods](#) section, and  $\gamma$  the cross-validated estimates of power in the broad  $\gamma$  band as described in the [Correlation analysis](#) section. Note that the causal analysis in this section is based on the SMR laterality score rather than on the SMR quality score that was employed for the correlation analysis in the preceding section. This is motivated by the consideration that the SMR quality score, being a function of the SMR laterality score and the true class label of the respective trial, is not an original brain signal, but rather an auxiliary variable that was constructed to identify brain signals correlated with SMR modulation. In the causal analysis, however, we wish to identify causal interactions between original brain signals and thus revert to the SMR laterality score. This score, being computed by a cross-validation procedure, is not confounded by the true class label of the respective trial, and thus constitutes an unconfounded measure of the SMR. The argument put forward in this section is based on the group-level analysis. Single-subject results are presented in [Supplementary Fig. 1](#).

In order to infer the causal structure that generated  $\mathcal{V}$ , we require the dependency structure between the elements of  $\mathcal{V}$ . This information can then be used to reject causal structures that are not in agreement with the observed dependency structure. Importantly, linear correlation test are not sufficient to obtain such a dependency structure, as these might fail to detect non-linear dependencies and may thus lead to incorrect causal conclusions. Accordingly, subsequent statistical independence tests utilize the non-linear HSIC independence test introduced in the [Methods](#) section.

First, we performed an HSIC test for determining dependence of  $c$  and  $\gamma$ . This test revealed that we cannot reject the null-hypothesis that  $c$  and  $\gamma$  were independent ( $p = 0.4415$ ,  $\text{HSIC} = 0.0542 \times 10^{-3}$ ,  $n = 3000$ ). Next, we tested  $c$  and  $\text{SMR}_i$ . An HSIC test rejected the null-hypothesis that  $c$  and  $\text{SMR}_i$  were independent with  $p = 9.998 \times 10^{-5}$  ( $\text{HSIC} = 26.9581 \times 10^{-3}$ ,  $n = 3000$ ). This is in agreement with the fact that we could infer  $c$  from  $\text{SMR}_i$  above chance level, as indicated by the classification accuracy score in the second column of Fig. 1. Third, we performed another HSIC test for determining dependence of  $\gamma$  and  $\text{SMR}_i$ . This test rejected the null-hypothesis that  $\gamma$  and  $\text{SMR}_i$  were independent with  $p = 1.9996 \times 10^{-4}$  ( $\text{HSIC} = 0.3924 \times 10^{-3}$ ,  $n = 3000$ ). We hence found strong evidence for a dependence between  $c$  and  $\text{SMR}_i$  as well as for a dependence between  $\text{SMR}_i$  and  $\gamma$ , as indicated by the highly significant  $p$ -values. Conversely, we found no support for a dependence between  $c$  and  $\gamma$ , with a  $p$ -value close to 0.5. Strictly, of course, the latter finding on its own cannot be interpreted as conclusive proof for independence, since it is impossible to quantify the evidence for the acceptance of a null-hypothesis in the same way as one can for its rejection. However, taken together these findings lead us to interpret the data as supporting independence of  $c$  and  $\gamma$ . Accordingly, we propose the dependency structure of  $\mathcal{V}$  to be given by  $c \leftrightarrow \text{SMR}_i \leftrightarrow \gamma$ , where the presence of a  $\leftrightarrow$  denotes an observed dependence relation.

It then remains to orient the arrows in a way that reflects the causal structure that generated  $\mathcal{V}$ . The first arrow between  $c$  and  $\text{SMR}_i$  can be oriented as  $c \rightarrow \text{SMR}_i$  by prior knowledge, since we know by virtue of the experimental paradigm that the instruction given to the

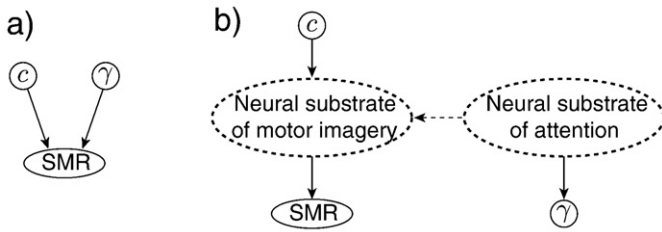


**Fig. 2.** Inferred causal graph (a) and proposed causal graph taking into account hidden variables (b). SMR denotes modulation of the sensorimotor rhythm (as measured by the SMR lateralization score),  $c$  denotes the type of motor imagery performed within each trial, and  $\gamma$  denotes global broad-band (55–85 Hz)  $\gamma$  power within each trial, weighted according to the spatial correlation structure as shown in the fifth column of Fig. 1.

subject is a cause of  $SMR_i$  and not vice versa. Concerning the causal relation between  $\gamma$  and  $SMR_i$ , note that if the causal structure that generated  $\mathcal{V}$  were given by  $c \rightarrow SMR_i \rightarrow \gamma$ , then  $\gamma$  and  $c$  would have to be dependent. Since our data provide no support for rejecting independence of  $c$  and  $\gamma$ , this strongly suggests the causal structure  $c \rightarrow SMR_i \leftarrow \gamma$  (Fig. 2.a). Accordingly, we propose that in the motor imagery paradigm considered in this study,  $\gamma$  rhythms had a causal influence on modulation of the SMR.

## Discussion

In this work, we have provided empirical evidence that  $\gamma$  rhythms have a causal influence on SMR modulation during motor imagery. As such, this study presents the first empirical evidence for a causal influence of  $\gamma$  oscillations on other brain rhythms, supporting the fundamental role attributed to  $\gamma$  rhythms for information processing within the brain.

To provide a more intuitive understanding of the discovered relation between  $\gamma$  oscillations and the SMR, Fig. 3 shows the actual values of the SMR lateralization score and  $\gamma$  power (as derived in the

Correlation analysis section) for all trials of subject S4. There are two important issues to note in this figure. First, it appears that the relation between the SMR lateralization score and  $\gamma$  power is quadratic, i.e., highly non-linear. This stresses the importance of the non-linear independence tests employed in the causal analysis, as a linear correlation analysis would have failed to detect this quadratic dependence. Second, it is noteworthy that the values of the SMR lateralization score of both conditions are densely clustered for low values of  $\gamma$  power, but are well separated across conditions for the high  $\gamma$  power regime. Accordingly, classification of trials as left or right hand motor imagery can be performed in subject S4 with almost perfect accuracy for high  $\gamma$  power, yet it is very unreliable for low  $\gamma$  power. While we have chosen to illustrate these issues on the subject showing the most prominent relation of  $\gamma$  power and the SMR lateralization score, the same (albeit more noisy) relations can also be identified on the group level.

Regarding the causal analysis, it should be noted that the conclusion of a causal influence of  $\gamma$  oscillations on the SMR assumed no hidden variables to be present. It is possible that both,  $\gamma$  oscillations and the SMR, are not causally effective themselves, but are generated by one or several unobserved causally effective processes. Indeed, it is sensible to assume that the SMR is generated by some neural substrate of motor imagery, while the observed  $\gamma$  rhythms are due to neuronal networks subserving attentional processes. This causal graph is shown in Fig. 2.b. Importantly though, even in this case the empirical evidence suggests that the attentional processes, giving rise to the  $\gamma$  rhythms, have a causal influence on the neural substrate of motor imagery: a reversed causal influence of the neural substrate of motor imagery on attentional processes would imply a dependence between  $c$  and  $\gamma$ , for which we found no empirical evidence.

Naturally, it is still possible to construct architectures that deliver the same results as those we observe, yet which are based on a causal structure of the form  $c \rightarrow SMR_i \rightarrow \gamma$ . For example, consider the causal model  $SMR_i = \theta_1 c + \epsilon_1$  and  $\gamma = \theta_2 |SMR_i| + \epsilon_2$ , for some constants-of-proportionality  $\theta$  and noise terms  $\epsilon$ . This model implies independence of  $c$  and  $\gamma$  despite a causal influence of  $SMR_i$  on  $\gamma$ . Note, however, that the formulation required to explain the data in this way has a very

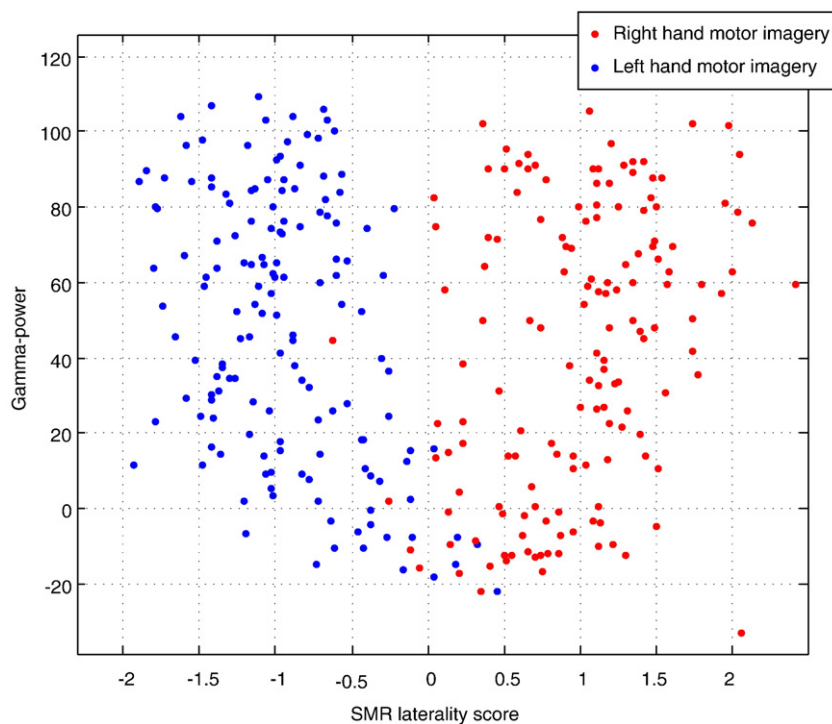


**Fig. 3.** Relationship of the SMR lateralization score and  $\gamma$  power (as derived in the Correlation analysis section) for subject S4 (dimensionless units). Each dot denotes one of a total of 300 trials.

specific parameterization, relative to the much larger class of mappings that can be chosen to explain the data given the causal structure  $c \rightarrow \text{SMR}_i \leftarrow \gamma$ . Occam's razor, also termed *stability* (Pearl, 2000) or *faithfulness* (Spirtes et al., 2000) in this context, therefore leads us to favor the latter.

In principle, further evidence for this causal structure could be provided by means of a multivariate analysis. As the causal structure  $c \rightarrow \text{SMR}_i \leftarrow \gamma$  implies the testable prediction that  $c$  and  $\gamma$ , though independent in a bivariate analysis, are dependent when conditioning on  $\text{SMR}_i$ , a conditional independence test could provide further support for a causal influence of  $\gamma$  oscillations on the SMR. Unfortunately, a linear multivariate analysis, e.g., as in a structural equation modeling framework, is not appropriate here due to the non-linear relation of  $\gamma$  power and the SMR laterality score. Non-linear conditional independence tests, on the other hand, are currently limited in their practicality by the requirement to partition (or in some way cluster) the variable to be conditioned on (cf. (Fukumizu et al., 2008) for recent work on non-linear conditional independence tests). Accordingly, non-linear conditional independence tests remain unreliable for limited amounts of data. Ultimately, only an interventional test, e.g., by neurofeedback programmes enabling volitional control of  $\gamma$  power, can prove a causal influence of  $\gamma$  rhythms on the SMR.

Regarding practical implications, our results are of particular significance for development of BCIs. As modulation of the SMR is typically used in BCIs to infer a subject's intention, our findings imply that  $\gamma$  oscillations have a causal influence on a subject's capability to utilize a BCI for means of communication. This may provide a means to address the problem of so-called "BCI-illiteracy" (Popescu et al., 2008): it is unknown why about 20% of all subjects are incapable of modulating their SMR sufficiently to achieve reliable communication by means of a BCI. Our results suggest that this incapability is (at least partially) caused by an insufficient shift of  $\gamma$  power from centro-parietal to frontal and, to a lesser extent, to occipital regions.

The behavioral correlate of this topographic alteration of  $\gamma$  power, however, remains unknown. Increased  $\gamma$  power over frontal areas has been associated with selective attention in auditory paradigms (Tiitinen et al., 1993) as well as with stimulus retention in short-term memory (Tallon-Baudry et al., 1998). Analogously, we speculate that the shift of  $\gamma$  power from centro-parietal to frontal and occipital regions reported here also reflects attentional processes. However, as this is the first report of the involvement of frontal  $\gamma$  oscillations in a motor-related paradigm, the specific role of this shift for motor imagery requires further investigation. Accordingly, we propose to provide subjects with feedback on the topographic distribution of  $\gamma$  power in order to determine the attentional processes associated with a shift of  $\gamma$  power from centro-parietal to frontal and occipital regions. These insights might then be used to provide BCI-illiterate subjects with specific instructions on how to alter the topographic distribution of  $\gamma$  power and hence enhance BCI-performance.

It is furthermore noteworthy that our results may help in the discrimination of *intentional-control* from *no-intentional-control* states (the latter meaning situations in which the user is not paying attention to the interface, or is taking time to think without wanting the interface to detect an action).

Finally, it is worth pointing out that the methodology employed here to uncover causal relations in brain imaging data can in principle be applied to a wide range of problems: if two brain processes  $A$  and  $B$  are found to be dependent, yet a set of experimental conditions  $C$  can

be found that affect only  $A$ , then this supports the hypothesis that  $B$  is a cause of  $A$  by means of the causal analysis employed in this study.

## Appendix A. Supplementary data

Supplementary data associated with this article can be found, in the online version, at doi:10.1016/j.neuroimage.2010.04.265.

## References

- Bauer, M., Oostenveld, R., Peeters, M., Fries, P., 2006. Tactile spatial attention enhances gamma-band activity in somatosensory cortex and reduces low-frequency activity in parieto-occipital areas. *J. Neurosci.* 26 (2), 490–501.
- Canolty, R., Edwards, E., Dalal, S., Soltani, M., Nagarajan, S., Kirsch, H., Berger, M., Barbaro, N., Knight, R., 2006. High gamma power is phase-locked to theta oscillations in human neocortex. *Science* 313, 1626–1628.
- Crone, N., Miglioretti, D., Gordon, B., Lesser, R., 1998. Functional mapping of human sensorimotor cortex with electrocorticographic spectral analysis – II. event-related synchronization in the gamma band. *Brain* 121, 2301–2315.
- Darvas, F., Miller, K., Rao, R., Ojemann, J., 2009. Nonlinear phase-phase cross-frequency coupling mediates communication between distant sites in human neocortex. *J. Neurosci.* 29 (2), 426–435.
- de Lange, F., Jensen, O., Bauer, M., Toni, I., 2008. Interactions between posterior gamma and frontal alpha/beta oscillations during imagined actions. *Front. Hum. Neurosci.* 2 (7), 1–12.
- Engel, A., Fries, P., Singer, W., 2001. Dynamic predictions: oscillations and synchrony in top-down processing. *Nat. Rev. Neurosci.* 2, 704–716.
- Fries, P., Nikolić, D., Singer, W., 2007. The gamma cycle. *TRENDS Neurosci.* 30 (7), 309–316.
- Fukumizu, K., Gretton, A., Sun, X., Schölkopf, B., 2008. Kernel measures of conditional dependence. In: Platt, J., Koller, D., Singer, Y., Roweis, S. (Eds.), *Advances in Neural Information Processing Systems*, vol. 20. MIT Press, pp. 489–496.
- Gretton, A., Fukumizu, K., Teo, C., Song, L., Schölkopf, B., Smola, A., 2008. A kernel statistical test for independence. In: Platt, J., Koller, D., Singer, Y., Roweis, S. (Eds.), *Advances in Neural Information Processing Systems*, vol. 20. MIT Press, pp. 585–592.
- Gruber, T., Müller, M., Keil, A., Elbert, T., 1999. Selective visual-spatial attention alters induced gamma band responses in the human EEG. *Clin. Neurophysiol.* 110 (12), 2074–2085.
- Jokisch, D., Jensen, O., 2007. Modulation of gamma and alpha activity during a working memory task engaging the dorsal or ventral stream. *J. Neurosci.* 27, 3244–3251.
- Mason, S., Bashashati, A., Fatourehchi, M., Navarro, K., Birch, G., 2007. A comprehensive survey of brain interface technology designs. *Ann. Biomed. Eng.* 35 (2), 137–169.
- McFarland, D., McCane, L., David, S., Wolpaw, J., 1997. Spatial filter selection for EEG-based communication. *Electroencephalogr. Clin. Neurophysiol.* 103, 386–394.
- Osipova, D., Hermes, D., Jensen, O., 2008. Gamma power is phase-locked to posterior alpha activity. *PLoS ONE* 3 (12), 1–7.
- Osipova, D., Takashima, A., Oostenveld, R., Fernández, G., Maris, E., Jensen, O., 2006. Theta and gamma oscillations predict encoding and retrieval of declarative memory. *J. Neurosci.* 26 (28), 7523–7531.
- Pearl, J., 2000. *Causality: Models, Reasoning, and Inference*. Cambridge University Press.
- Pfurtscheller, G., Graimann, B., Huggins, J., Levine, S., Schuh, L., 2003. Spatiotemporal patterns of beta desynchronization and gamma synchronization in corticographic data during self-paced movement. *Clin. Neurophysiol.* 114, 1226–1236.
- Pfurtscheller, G., Neuper, C., 2001. Motor imagery and direct brain-computer communication. *Proc. IEEE* 89 (7), 1123–1134.
- Popescu, F., Blankertz, B., Mueller, K., 2008. Computational challenges for noninvasive brain computer interfaces. *IEEE Intell. Syst.* 23 (3), 78–79.
- Schölkopf, B., Smola, A., Williamson, R., Bartlett, P., 2000. New support vector algorithms. *Neural Comput.* 12, 1207–1245.
- Sederberg, P., Schulze-Bonhage, A., Madsen, J., Bromfield, E., McCarthy, D., Brandt, A., Tully, M., Kahana, M., 2007. Hippocampal and neocortical gamma oscillations predict memory formation in humans. *Cereb. Cortex* 17, 1190–1196.
- Sokolov, A., Pavlova, M., Lutzenberger, W., Birbaumer, N., 2004. Reciprocal modulation of neuromagnetic induced gamma activity by attention in the human visual and auditory cortex. *NeuroImage* 22 (2), 521–529.
- Spirtes, P., Glymour, C., Scheines, R., 2000. *Causation, Prediction, and Search*. MIT Press.
- Tallon-Baudry, C., Bertrand, O., 1999. Oscillatory gamma activity in humans and its role in object representation. *Trends Cogn. Sci.* 3 (4), 151–162.
- Tallon-Baudry, C., Bertrand, O., Peronnet, F., Pernier, J., 1998. Induced gamma-band activity during the delay of a visual short-term memory task in humans. *J. Neurosci.* 18 (11), 4244–4254.
- Tallon-Baudry, C., Kreiter, A., Bertrand, O., 1999. Sustained and transient oscillatory responses in the gamma and beta bands in a visual short-term memory task in humans. *Vis. Neurosci.* 16, 449–459.
- Tiitinen, H., Sinkkonen, J., Reinikainen, K., Alho, K., Lavikainen, J., Näätänen, R., 1993. Selective attention enhances the auditory 40-Hz transient response in humans. *Nature* 364, 59–60.